Optics Letters

Temperature-dependent excitonic photoluminescence excited by two-photon absorption in perovskite $CsPbBr_3$ quantum dots

Ke Wei,[1] Zhongjie Xu,[1,2] Runze Chen,[2] Xin Zheng,[2] Xiangai Cheng,[1,2] and Tian Jiang[1,2,3,*]

[1]College of Opto-Electronic Science and Engineering, National University of Defense Technology, Changsha 410073, China
[2]State Key Laboratory of High Performance Computing, National University of Defense Technology, Changsha 410073, China
[3]State Key Laboratory of Low-Dimensional Quantum Physics, Department of Physics, Tsinghua University, Beijing 10000, China
*Corresponding author: tjiang@nudt.edu.cn

Received 11 July 2016; accepted 19 July 2016; posted 21 July 2016 (Doc. ID 268661); published 9 August 2016

Recently, lead halide perovskite quantum dots have been reported with potential for photovoltaic and optoelectronic applications due to their excellent luminescent properties. Herein excitonic photoluminescence (PL) excited by two-photon absorption in perovskite $CsPbBr_3$ quantum dots (QDs) has been studied at a broad temperature range, from 80 to 380 K. Two-photon absorption has been investigated and the absorption coefficient is up to 0.085 cm/GW at room temperature. Moreover, the PL spectrum excited by two-photon absorption shows a linear blue-shift (0.32 meV/K) below the temperature of 220 K. However, for higher temperatures, the PL peak approaches a roughly constant value and shows temperature-independent chromaticity up to 380 K. This behavior is distinct from the general red-shift for semiconductors and can be attributed to the result of thermal expansion, electron–phonon interaction and structural phase transition around 360 K. The strong nonlinear absorption and temperature-independent chromaticity of $CsPbBr_3$ QDs observed in temperature range from 220 to 380 K will offer new opportunities in nonlinear photonics, light-harvesting, and light-emitting devices.

OCIS codes: (260.2510) Fluorescence; (190.4400) Nonlinear optics, materials; (160.4760) Optical properties; (160.4236) Nanomaterials.

http://dx.doi.org/10.1364/OL.41.003821

Semiconductor quantum dots (QDs) have been intensively studied for size- and surface-dependent properties [1] and various applications on optoelectronic devices [2–6]. Previous reports were mostly concentrated on binary and multinary (ternary, quaternary) metal chalcogenide nanocrystals [7,8]. In recent years, lead halide perovskite QDs ($MPbX_3$. $M = CH_3NH_3$, Cs; X = Cl, Br, I) have been reported as a new family of nanomaterials. Simple change of the composition or the size of QDs can continuously tune the bandgap over entire visible spectrum [9–11]. The excitonic emission presents high photoluminexcence (PL) quantum yields (QYs), narrow peak, and temperature-independent chromaticity. These excellent optical properties make perovskite QDs a promising alternative for light-harvesting and lightemitting applications [12,13]. Moreover, recent reports by Kovalenko's [6] and Sun's [14,15] groups show that the $CsPbBr_3$ QDs have strong nonlinear absorption and low-threshold stimulated emission, which will offer potential applications on low-cost nonlinear absorbers and optical gain media.

To date, most research on $CsPbBr_3$ QDs has been carried out at room temperature. However, it is well-known that the bandgap of semiconductors is temperature-dependent [16,17]. Recently, a small blue-shift (0.035 meV/K) of the excitonic PL peak in $CsPbBr_3$ nanowire was found at temperatures ranging from 5.8 to 295 K [18], which was attributed to the competition of lattice expansion and electron–phonon (EP) coupling. However, $CsPbBr_3$ QDs was only studied from 298 to 373 K and it was found that the optical bandgap was independent of temperature [19], which is quite different from $CsPbBr_3$ nanowire and other semiconductors. The anomalous behavior of the bandgap of perovskite $CsPbBr_3$ QDs is not yet well understood.

In this Letter, stable-state and time-resolved PL excited by two-photon absorption in perovskite $CsPbBr_3$ QDs are studied at a wide temperature range, from 80 to 380 K. A two-photon absorption coefficient is found up to 0.085 cm/GW at room temperature. For the temperature below 220 K, the peak of PL spectrum increases linearly (0.32 meV/K) with increasing temperature, indicating that thermal expansion (TE) dominates the bandgap behavior. For higher temperatures, a roughly stable PL peak is found resulting from TE, EP interaction, and the structural phase transition.

$CsPbBr_3$ QDs are synthesized, as previously reported [10]. Figure 1(a) shows a transmission electron microscopy (TEM) image of the colloidal QDs (solvent of toluene). The edge length is summarized in Fig. 1(b), with an average size of 11.4 nm, which is comparable to the estimated bulk Bohr exciton diameter [10]. So, a quantum confined effect leads to blue-shift of the bandgap compared to its bulk counterpart. As shown in the linear absorption spectrum [Fig. 1(c)], the

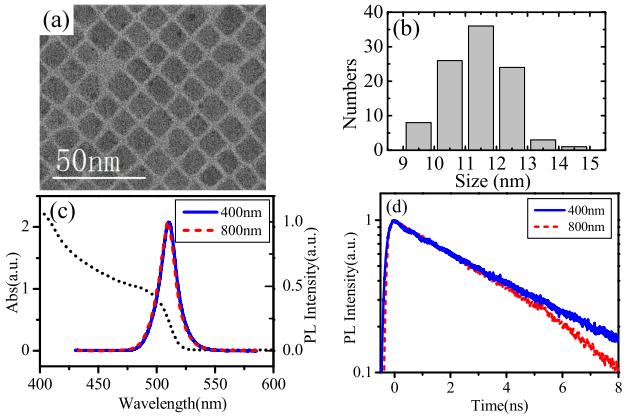

Fig. 1. Characterization of $CsPbBr_3$ QDs. (a) and (b) TEM image and statistical distributions of the edge length. (c) Linear absorption (dot) and PL excited by 400 nm (solid line) and 800 nm (dashed line) laser. (d) PL decay excited by 400 nm (solid line) and 800 nm (dashed line) laser.

lowest energy excitonic band is centered at 500 nm, which is consistent with previous reports [10]. Room temperature PL excited by both 400 and 800 nm femtosecond lasers is centered at 513 nm, with full width at half-maximum (FWHM) of 81 meV. The PL QYs are estimated to be ~88% by integrating sphere measurements. The PL excited by an 800 nm laser indicates that the $CsPbBr_3$ QDs are indeed multiphoton active [14]. The PL decay is also measured by the method of time-correlated single photon counting (TCSPC), with an instrument response function (IRF) of 200 ps (FWHM). As shown in Fig. 1(d), for both the 400 and 800 nm excitations, most of the excitons decay with a single-exponential time constant of ~4 ns. The single-exponential PL decay in conjunction with the high PL QYs indicates small trapping states in the $CsPbBr_3$ QDs.

For more insights into the nonlinear absorption of $CsPbBr_3$ QDs, excitation density-dependent PL spectrum measurement is carried out, as shown in Fig. 2(a). The sample is held in a rotating sapphire curvette to ensure the uniform distribution of QDs and prevent the optical tweezers effect. The integrated PL intensity is extracted in Fig. 2(b), which exhibits almost quadratic relationship with excitation density. Since excitation of an exciton (electron-hole pair) through two-photon absorption needs to simultaneously absorb two photons through a virtual state, as shown in the inset of Fig. 2(b), this quadratic dependence clearly shows two-photon absorption in the QDs.

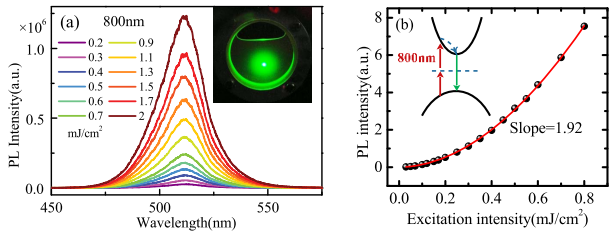

Fig. 2. (a) PL spectrum under different excitation densities at room temperature. The inset shows the photograph of colloidal $CsPbBr_3$ QDs illuminated by an 800 nm laser beam. (b) Integrated PL intensity as a function of excitation intensity. The inset shows the schematic of two-photon absorption.

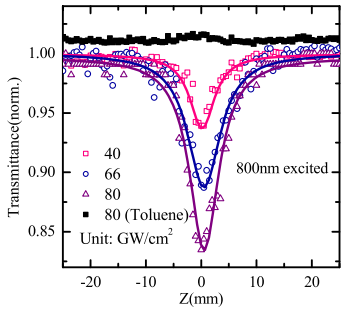

Fig. 3. Open aperture Z-scan measurement for $CsPbBr_3$ QDs and the pure solvent (toluene) at different excitation intensities (at focus). The solid lines show the best fits using Z-scan theory.

To quantitatively describe the two-photon absorption, Z-scan measurement is carried out. Details of the setup can be found in Ref. [20]. As shown in Fig. 3, no obvious response of the toluene solvent is observed, even in the maximum intensity used in the measurements. So the signal generates mainly from $CsPbBr_3$ QDs. The reverse saturable absorption (RSA) signal in all excitation intensities higher than 40 GW/cm^2 clearly shows nonlinear absorption in the QDs. By fitting the experimental data with Z-scan theory [20], a two-photon absorption coefficient is obtained up to ~0.085 cm/GW, which is comparable to a recent report of $CsPbBr_3$ nanocrystals [14].

In order to perform an in-depth analysis of the exciton generated by two-photon absorption, the $CsPbBr_3$ QDs solution is dripped on an ultrathin glass substrate, and the stable-state PL spectrum is measured under different temperatures from 80 to 380 K, as shown in Fig. 4. To ensure the single-exciton process during carrier relaxation, the excitation intensity (800 nm) is adjusted to as low as 0.08 mJ/cm^2, at which no saturation of PL intensity is found [Fig. 2(b)]. Importantly, no significant difference of the PL spectrum is found at the same temperature during the cooling and heating process.

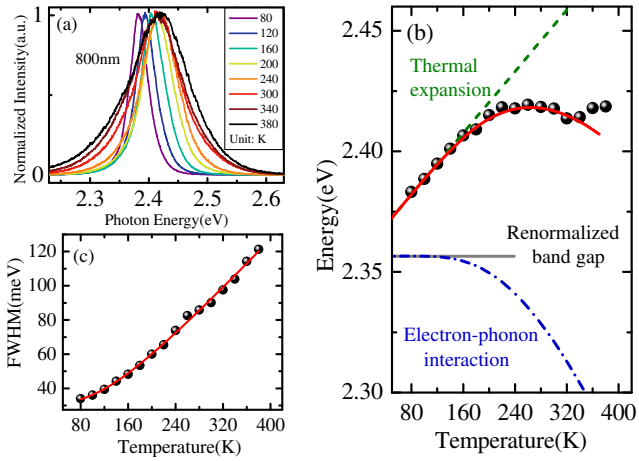

Fig. 4. (a) Temperature-dependent PL spectrum excited by an 800 nm laser beam, all normalized to clarify the peak shift. (b) Corresponding PL peak. The solid line is the fit according to Eq. (3); the dashed and the dashed–dotted line show the individual contributions of TE and EP interaction. (c) Linewidth of the PL spectrum. The solid line is the fit according to Eq. (4).

As summarized in Fig. 4(b), the PL peak shows a linear blue-shift with increasing temperatures below 220 K, which is opposite to common semiconductors. A similar blue-shift is also observed in $CsPbBr_3$ nanowires [18], $CH_3NH_3PbI_3-xCl_x$ films [21], $CsSnI_3$ [22], and Pb-doped CsBr crystals [23]. For higher temperatures, the PL peaks shows a roughly constant value (fluctuation < 1 nm). This temperature-independent chromaticity is also observed in recent research of $CsPbBr_3$ QDs [19]. Chromaticity under different temperatures is a very important parameter for applications such as light-emitting diodes, which often heat up during prolonged operation. The almost constant PL peak of $CsPbBr_3$ QDs in such a broad temperature range from 220 to 380 K makes it particularly suited to light-emitting devices.

Although the PL peak seems to be constant from 220 to 380 K, small but regular shifts can be found after careful examination and repeated experiments. The PL peak slightly decreases from 260 to 340 K and increases from 340 to 380 K, forming a very shallow trough with fluctuation less than 1 nm around 340 K. Most efforts are concentrated on this interesting behavior in the rest of this Letter.

At constant pressure, the temperature-dependence of the bandgap is generally estimated by the following expression under a quasi-harmonic approximation [22]:

$$\frac{\partial E_g}{\partial T}=\frac{\partial E_g}{\partial V}\frac{\partial V}{\partial T}+\sum_{j,\vec{q}}\left(\frac{\partial E_g}{\partial n_{j,\vec{q}}}\right)\left(n_{j,\vec{q}}+\frac{1}{2}\right), \quad (1)$$

where $n_{j,\vec{q}}$ is the number of phonons at j branch with wave vector of $\vec{q}$, and it follows the Bose–Einstein distribution

$$n_{j,\vec{q}}=\frac{1}{\exp(\hbar\omega_{j,q}/k_BT)-1}, \quad (2)$$

where $\omega_{j,\vec{q}}$ is the angular frequency of the phonon mode. The first part of Eq. (1) describes the contribution of the TE of the lattice. The coefficient $\partial E_g/\partial V$ depends weakly on temperature and thus can be regarded as a constant. Its value can be either positive or negative, depending on the specifics of the bonding parameters as well as the detailed structure of the bandgap [22]. Band structure calculation of $CsSnBr_3$ [24] shows that the valence band maximum (VBM) is the hybridization between the p orbit of Br and s orbit of Sn. With increased temperature, TE of the lattice will decrease the interaction between these two orbits, resulting in a decrease of the valance bandwidth and an increase of the bandgap. Similar behavior is hypothesized for $CsPbBr_3$ QDs. So here, the $\partial E_g/\partial V$ is determined to be positive.

The second part of Eq. (1) is attributed to the EP interaction. Since it is a challenging task to calculate all the possible phonon modes in an entire Brillouin zone, many models have been developed to interpret the experimental data, such as the one- and two-oscillator models [25], in which only one and two dominant phonon modes are considered. The two-oscillator models are usually used to fit the nonmonotonic temperature-dependent bandgap, which usually shows a nonlinear temperature dependence at low temperature and a linear one at high temperature, while in $CsPbBr_3$ QDs, the linear increase followed by a roughly constant value of the bandgap does not conform to the two-oscillator model. So the one-oscillator model is considered here. Combined with the TE, Eq. (1) can be simplified to the following expression by assuming a linear relationship between lattice constant and temperature:

$$E_g(T)=E_0+A_{\mathrm{TE}}T+A_{\mathrm{EP}}\left(\frac{2}{\exp(\hbar\omega/k_BT)-1}+1\right), \quad (3)$$

where E_0 is the unrenormalized bandgap, A_{TE} and A_{EP} are the weight of the TE and EP interaction, respectively, and $\hbar\omega$ is the average optical phonon energy. Due to the quantum factor in the phonon distribution function, there is an energy correction of the bandgap even at zero temperature, namely $E_g(T=0)=E_0+A_{\mathrm{EP}}$.

Fitting the temperature-dependent PL peak with Eq. (3), the parameters are obtained: $E_0=2.8(1)$eV, $A_{\mathrm{TE}}=0.32(2)$ meV/K, $A_{\mathrm{EP}}=-400(100)$meV, and $\hbar\omega=80(10)$meV. Figure 4(b) shows the fitting results. To highlight the contribution of the TE and the EP interaction, both of them are added to the renormalized bandgap ($E_g(T=0)$). It clearly shows that the linear-increased PL peak can be derived from the domination of TE below 220 K, while EP interaction is negligible due to the unsubstantially populated optical phonon modes. However, for higher temperatures, the optical phonon modes are appreciably populated, leading to an increasingly negative contribution, as shown by the blue dashed–dotted line in Fig. 4(b). So the increasing rate of the PL peak is slowed down, and even reversed from 260 ~ 340 K. If no other factors contribute to the bandgap behavior, the energy of PL peak is still expected to decrease at higher temperatures than 340 K. However, an opposite behavior is obtained. Previous reports [19,26] reveal an occurrence of structural phase transition from orthorhombic to tetragonal in $CsPbBr_3$ around 360 K. Such phase transition will lead to a renormalization of bandgap, as the case of hybrid organometal halide perovskite films [21,27]. So the increase of PL peak from 340 to 380 K is attributed to such phase transition.

As shown in Fig. 4(c), the PL linewidth (FWHM) broadens monotonously with increasing temperature, which can be commonly described using the following model [28]:

$$\Gamma(T)=\Gamma_0+\Gamma_{\mathrm{photon}}(e^{\hbar\omega_{\mathrm{LO}}/k_BT}-1)^{-1}+\Gamma_{\mathrm{imp}}e^{-E_b/k_BT}, \quad (4)$$

where Γ_0 is the inhomogeneous broadening contribution. Γ_{photon} and $\hbar\omega_{\mathrm{LO}}$ represent the coupling strength and energy of the longitudinal optical phonon, respectively. One should note that although the EP coupling is not expected to dominate the behavior of the bandgap below 220 K, it does exist and contribute to the broadening of PL linewidth. The third part is attributed to ionized impurity scattering, which can be neglected in $CsPbBr_3$ QDs due to the negligible trap states, as described above. From the fitting process, the parameters are estimated as follows: $\Gamma_0=32(2)$meV, $\Gamma_{\mathrm{photon}}=130(20)$meV, and $\hbar\omega_{\mathrm{LO}}=30(3)$meV. The fitting optical phonon energy is much lower than the average optical phonon energy [80(10)meV] contributed to the bandgap behavior. The origin of this difference needs to be further studied.

Finally, to reconfirm the above model, temperature-dependent PL lifetime measurement is carried out, as shown in Fig. 5. The lifetime increases monotonically below room temperature and shows a maximum (2.4 ns) at ~300 K, roughly agreeing with the behavior of the PL peak [Fig. 4(b)]. The 2.4 ns PL lifetime of the coagulated $CsPbBr_3$ QDs on the glass is slightly shorter than 4 ns of the solution one [as shown in Fig. 1(d)], probably due to the increase of the surface state when the QDs

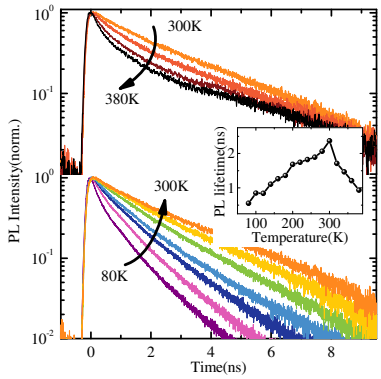

Fig. 5. Temperature-dependent PL decay excited by an 800 nm laser beam. The inset extracts the effective PL lifetime.

are coagulated on the glass substrate. More theoretical and experimental studies are required for a better understanding of this behavior.

For temperature below 300 K, due to weak EP interaction, the nonradiative recombination is relatively small, and the radiative recombination of single exciton state dominates the carrier decay. Thus with increasing temperature, thermal motion becomes more active and thus prevents the recombination of excitons, resulting in an increase of PL lifetime, as shown in the lower column of Fig. 5, while for temperature higher than 300 K, as shown in upper column of Fig. 5, the increasing EP interaction will drastically increase the nonradiative recombination and reduce the PL lifetime. This behavior is commonly known as thermal quenching. On the other hand, the transition from exponential to nonexponential decay at 300 K also indicates an increasing nonradiative process in $CsPbBr_3$ QDs.

In conclusion, excitonic PL excited by two-photon absorption in $CsPbBr_3$ QDs is studied at a wide temperature range, from 80 to 380 K, by steady and time-resolved PL spectroscopy and Z-scan measurement. A two-photon absorption coefficient is found up to 0.085 cm/GW at room temperature. The energy of PL peak increases linearly below 220 K and approaches a roughly constant value at 220 K ~ 380 K. Theoretical research reveals that TE is expected to dominate the bandgap behavior below 220 K, leading to a linear positive dependent optical bandgap, while for temperature higher than 220 K, due to the competition between TE and EP interaction, the increase rate is slowed down, and even slightly reversed from 260 to 340 K. The occurrence of structural phase transition from orthorhombic to tetragonal leads to a small blue-shift of the PL peak at temperatures higher than 340 K. Overall, the fluctuation of PL peak is less than 1 nm from 220 K ~ 380 K. This complex bandgap behavior is also conformed to that of PL lifetime, which indicates a balance between thermal motion and EP interaction at ~300 K. The strong nonlinear absorption and the luminescence monochromaticity at such a wide temperature range from 220 K to 380 K make the $CsPbBr_3$ QDs a promising material in low-cost nonlinear absorbers, light-harvesting, and light-emitting applications.

Funding. Scientific Researches Foundation of College of Optoelectronic Science and Engineering; National University of Defense Technology (0100070014007).

REFERENCES

1. A. Rogach, ACS Nano **8**, 6511 (2014).
2. E. H. Sargent, Nat. Photonics **3**, 325 (2009).
3. I. J. Kramer and E. H. Sargent, Chem. Rev. **114**, 863 (2013).
4. Q. Sun, Y. A. Wang, L. S. Li, D. Wang, T. Zhu, J. Xu, C. Yang, and Y. Li, Nat. Photonics **1**, 717 (2007).
5. J. M. Caruge, J. E. Halpert, V. Wood, V. Bulović, and M. G. Bawendi, Nat. Photonics **2**, 247 (2008).
6. S. Yakunin, L. Protesescu, F. Krieg, M. I. Bodnarchuk, G. Nedelcu, M. Humer, G. D. Luca, M. Fiebig, W. Heiss, and M. V. Kovalenko, Nat. Commun. **6**, 8056 (2015).
7. O. Chen, J. Zhao, V. P. Chauhan, J. Cui, C. Wong, D. K. Harris, H. Wei, H. Han, D. Fukumura, and R. K. Jain, Nat. Mater. **12**, 445 (2013).
8. D. Aldakov, A. Lefrançois, and P. Reiss, J. Mat. Chem. C **1**, 3756 (2013).
9. H. Huang, A. S. Susha, S. V. Kershaw, T. F. Hung, and A. L. Rogach, Adv. Sci. **2**, 1500194 (2015).
10. L. Protesescu, S. Yakunin, M. I. Bodnarchuk, F. Krieg, R. Caputo, C. H. Hendon, R. X. Yang, A. Walsh, and M. V. Kovalenko, Nano Lett. **15**, 3692 (2015).
11. Q. A. Akkerman, V. D. Innocenzo, S. Accornero, A. Scarpellini, A. Petrozza, M. Prato, and L. Manna, J. Am. Chem. Soc. **137**, 10276 (2015).
12. J. Song, J. Li, X. Li, L. Xu, Y. Dong, and H. Zeng, Adv. Mater. **27**, 7161 (2015).
13. J. H. Im, C. R. Lee, J. W. Lee, S. W. Park, and N. G. Park, Nanoscale **3**, 4088 (2011).
14. Y. Wang, X. Li, X. Zhao, L. Xiao, H. Zeng, and H. Sun, Nano Lett. **16**, 448 (2015).
15. Y. Wang, X. Li, J. Song, L. Xiao, H. Zeng, and H. Sun, Adv. Mater. **27**, 7101 (2015).
16. E. Poliani, M. Bonfanti, M. Guzzi, E. Grilli, M. Gurioli, N. Koguchi, and S. Sanguinetti, Phys. Rev. B **73**, 125342 (2006).
17. M. Schwab, M. Bayer, R. Pässler, S. Fafard, Z. Wasilewski, P. Hawrylak, A. Forchel, and G. Ortner, Phys. Rev. B **72**, 85328 (2005).
18. D. Zhang, S. W. Eaton, Y. Yu, L. Dou, and P. Yang, J. Am. Chem. Soc. **137**, 9230 (2015).
19. A. Swarnkar, R. Chulliyil, V. K. Ravi, M. Irfanullah, A. Chowdhury, and A. Nag, Angew. Chem. Int. Ed. **54**, 15424 (2015).
20. X. Zheng, R. Chen, G. Shi, J. Zhang, Z. Xu, and T. Jiang, Opt. Lett. **40**, 3480 (2015).
21. W. Kewei, B. Ashok, M. Chun, D. Yuanmin, Y. Yang, L. Liang, and W. Tom, Phys. Chem. Chem. Phys. **16**, 22476 (2014).
22. C. Yu, Z. Chen, J. J. Wang, W. Pfenninger, N. Vockic, J. T. Kenney, and K. Shum, J. Appl. Phys. **110**, 63526 (2011).
23. R. Aceves, V. Babin, M. B. Flores, P. Fabeni, A. Maaroos, M. Nikl, K. Nitsch, G. P. Pazzi, R. P. Salas, and I. Sildos, J. Lumin. **93**, 27 (2001).
24. L. Huang and W. R. Lambrecht, Phys. Rev. B **88**, 165203 (2013).
25. J. P. Brison, H. Suderow, P. Rodière, A. Huxley, S. Kambe, F. Rullier-Albenque, and J. Flouquet, Phys. Rev. B **86**, 195208 (2012).
26. K. S. Aleksandrov, Ferroelectrics **14**, 801 (1976).
27. R. L. Milot, G. E. Eperon, H. J. Snaith, M. B. Johnston, and L. M. Herz, Adv. Funct. Mater. **25**, 6218 (2015).
28. J. Lee, E. S. Koteles, and M. O. Vassell, Phys. Rev. B **33**, 5512 (1986).